# 6A.3 A NEW LATENT HEAT FLUX PARAMETERIZATION FOR LAND SURFACE MODELS

Christopher M. Godfrey*
University of Oklahoma, Norman, Oklahoma

David J. Stensrud
NOAA/National Severe Storms Laboratory, Norman, Oklahoma

Lance M. Leslie
University of Oklahoma, Norman, Oklahoma

## 1. INTRODUCTION

Numerical weather prediction models require an accurate representation of initial land surface conditions in order to partition properly the sensible and latent heat fluxes that drive the evolution of the planetary boundary layer. Several key components of the land surface that significantly affect surface heat and moisture fluxes include soil temperature and moisture, fractional vegetation coverage ($\sigma_f$), and green leaf area index (LAI). The lack of observational data for the accurate specification of these components in model initial conditions is arguably the most difficult aspect in the evaluation of land surface models. Routine observations of $\sigma_f$ and LAI are not available at high resolution ($\sim$1 km), nor are soil moisture and soil temperature. This gap in our observational capabilities seriously hampers the evaluation and improvement of land surface model parameterizations, since improper initial conditions and inaccuracies in the model formulations very likely produce comparable model errors.

Models accomplish the exchange of energy between the land surface and the atmosphere through land surface parameterizations (e.g., Bhumralkar 1975; Blackadar 1976; Deardorff 1978; McCumber and Pielke 1981; Pan and Mahrt 1987; Noilhan and Planton 1989), which characterize the state of the land surface and forecast the evolution of the lowest layer of the model atmosphere. The surface energy balance relies strongly upon the soil and near-surface conditions, and plays a critical role in determining the prognostic variables in land surface models. Surface energy fluxes depend heavily upon soil temperature and soil moisture conditions, as well as vegetation coverage, atmospheric conditions, and the physical properties of the soil. Soil moisture is an important component describing the land surface and provides a key link between the atmosphere and the water and energy balances at the surface of the earth (Wei 1995; Robock et al. 2000; Leese et al. 2001). It influences the available water for plant transpiration, and plays a role in the mass balance for many forecast models. Soil thermal conductivity estimates, which facilitate the proper heat transfer within the soil, also strongly depend upon soil moisture specifications. For calculations of soil heat transfer, the most sophisticated land surface parameterizations require not only near-surface soil temperatures, but also temperature profiles within the soil (e.g., Viterbo and Beljaars 1995; Chen and Dudhia 2001). In addition, vegetation coverage and density provide critical information on the partitioning of total evaporation between bare soil and canopy transpiration (Chen and Dudhia 2001). Together, soil temperature, soil moisture, and vegetation affect forecasts of temperature, mixing ratio, cloud cover, and precipitation by working in concert to directly influence sensible, latent, and ground heat fluxes.

The mesoscale model employed for this study implements a monthly climatology for fractional vegetation coverage and a constant leaf area index. Studies have shown that such coarse resolution data based solely on climatology are insufficient to capture the detailed surface characteristics necessary to properly initialize a land surface parameterization (e.g., Chang and Wetzel 1991; Crawford et al. 2001; Santanello and Carlson 2001; Kurkowski et al. 2003). By using climatological values for land surface characteristics, the model does not account for short-term or annual variability in vegetation coverage and condition due to daily variations in rainfall, seasonal droughts, flooding, forest fires, irrigation, deforestation, desertification, crop harvesting, land usage, hail or tornado damage, and temporal variations in the growth and senescence of green vegetation. Large-scale atmospheric oscillations may also play a role in the interannual variability of vegetation (e.g., Jin and Zhang 2002; Matsui et al. 2005). Modeling studies implementing near real-time land surface characteristics from satellite observations have shown great promise for improving forecasts (e.g., Oleson and Bonan 2000; Zeng et al. 2000; Crawford et al. 2001; Kurkowski et al. 2003).

Taking advantage of a unique set of soil and vegetation observations to improve the initial specification of the land surface should lead to more accurate model forecasts of air temperature and moisture, which directly affect planetary boundary layer processes and convective development. A modified version of The Pennsylvania State University–National Center for Atmospheric Research (PSU–NCAR) fifth-generation Mesoscale Model (MM5) version 3.6 (Dudhia 1993; Grell et al. 1995; Dudhia 2003) assimilates soil temperature, soil moisture, $\sigma_f$, and LAI observations for several case studies. In addi-

*Corresponding author address: Christopher M. Godfrey, University of Oklahoma, School of Meteorology, 120 David L. Boren Blvd., Suite 5900, Norman, Oklahoma 73072; e-mail: christopher.godfrey@noaa.gov.

tion to supplying initial soil conditions, a dense network of surface observations over the primary study area provides a means to verify model forecasts. Results show that despite improved land surface conditions, inaccuracies still exist in the model formulations (Godfrey et al. 2005). This result provides a springboard for assessing parameterization errors within the model. As a first step in assessing errors in the surface energy balance, the current study introduces a new empirical latent heat flux parameterization. In a novel approach to determining latent heat flux, the new parameterization derives from surface observations rather than from theoretical formulations.

## 2. DATA

The Oklahoma Mesonet is an integrated network of automated surface observing stations, with at least one site in each of Oklahoma's seventy-seven counties. Measurements of atmospheric variables occur every five minutes at each of the 116 sites. All Mesonet sites report soil temperature at one or more depths every fifteen minutes. Over 100 sites also record soil moisture every thirty minutes at levels of 5, 25, 60, and 75 cm below the surface. Approximately 75 sites measure ground heat flux and total net radiation every five minutes. A special suite of instruments augments the standard instrumentation at ten sites, measuring sensible heat flux and the four components of net radiation every five minutes. All data fall subject to rigorous quality assurance procedures in order to produce reliable research-quality data (Shafer et al. 2000). A complete description of the Oklahoma Mesonet, including sensor specifications, appears in Brock et al. (1995). Basara and Crawford (2000) describe the soil moisture instrumentation and Brotzge et al. (1999) discuss the surface energy flux measurements.

Vegetation indexes originate from daily updates of National Oceanic and Atmospheric Administration (NOAA) Advanced Very High Resolution Radiometer (AVHRR) normalized difference vegetation index (NDVI) data. Godfrey et al. (2005) describe the derivation of $\sigma_f$ and LAI from NDVI observations.

## 3. LATENT HEAT FLUX IN THE NOAH LSM

The National Centers for Environmental Prediction–Oregon State University–Air Force–Hydrologic Research Lab (Noah) land surface model (LSM, Chen et al. 1996; Koren et al. 1999) is the primary driver for land surface processes in the Eta, Weather Research and Forecasting (WRF), and MM5 forecast models. Preliminary tests show that forecasts by the Noah LSM consistently underestimate midday latent heat fluxes by 20–40% compared with observations on clear days with weak synoptic forcing, even when given the best possible characterization of the initial land surface conditions. These errors primarily result from errors in the partitioning between the fluxes of sensible and latent heat. Partitioning errors can arise from a number of problems, including incorrect estimates of moisture availability, skin temperature, and resistance to heat flux, which is a function of air temperature and the vertical separation of atmospheric model layers. Improving surface fluxes may lead to better surface and boundary layer temperature and moisture forecasts, which will increase predictability (e.g., Crook 1996).

More complicated factors influence latent heat fluxes compared with sensible heat fluxes, exacerbating the difficulty of modeling evaporation near the land surface. However, surface observations under a variety of atmospheric conditions may aid in appropriately tuning the latent heat flux. In the current formulation within the Noah LSM, the latent heat flux $E$ is the sum of the contribution from each of three types of evaporation: direct evaporation from bare soil ($E_{\rm dir}$), transpiration from the vegetation canopy and roots ($E_t$), and evaporation of precipitation intercepted by the vegetation canopy ($E_c$). All three of these terms depend directly on the calculation of potential evaporation.

### 3.1 *Potential evaporation*

The potential evaporation $E_p$ is the maximum possible evaporation that could occur over an open water surface under existing atmospheric conditions. The Noah LSM calculation for potential evaporation involves an energy balance approach based on the Penman relationship (Penman 1948) and includes a stability-dependent aerodynamic resistance term (Mahrt and Ek 1984). Since calculation of the net radiation in the model requires knowledge of the surface temperature, the actual set of equations in the model differs slightly from the usual Penman relationship and the equation for potential evaporation appearing in Mahrt and Ek (1984). This results in

$$E_p = \frac{\rho c_p C_h}{L_v}\left(\frac{\Delta\left[\frac{R_n}{\rho c_p C_h}+\left(\theta_0 - T_0\right)\right]+A(r+1)}{\Delta+r+1}\right), \qquad (1)$$

where $\rho$ is the air density, $c_p$ is the specific heat at constant pressure, and $\theta_0$ and $T_0$ are the potential and actual temperatures at the lowest model level, respectively,

$$R_n = (1-\alpha)R_g + L_d - \sigma T_0^4 - G, \qquad (2)$$

is the net radiation (W m$^{-2}$), where $\alpha$ is the surface albedo, $R_g$ is the incoming solar radiation, $L_d$ is the downward longwave radiation, $G$ is the ground heat flux, and $\sigma$ is the Stefan-Boltzmann constant,

$$\Delta = \frac{dq_s}{dT}\frac{L_v}{c_p}, \qquad (3)$$

where $dq_s/dT$ is the slope of the saturation specific humidity curve with respect to temperature and $L_v$ is the latent heat of vaporization,

$$r = \frac{4\sigma T_0^4 R_d}{p_{\rm sfc} c_p C_h}, \qquad (4)$$

where $R_d$ is the dry gas constant and $p_{\text{sfc}}$ is the surface pressure (Pa), and

$$A = \frac{L_v}{c_p}\left(q_s\left(T_0\right) - q_0\right), \tag{5}$$

where $q_0$ and $q_s(T_0)$ are the actual and saturation specific humidities at the model level closest to the ground surface, respectively (Ek and Mahrt 1991). Here $C_h$ is the surface exchange coefficient for heat and momentum, the definition of which varies depending upon the stability of the lower atmosphere, and is a function of the wind speed and height above the surface at the first model level, the roughness lengths for momentum and heat, and the bulk Richardson number for the surface layer. For details of the calculation of $C_h$, see Mahrt and Ek (1984) and Ek and Mahrt (1991). Note that in the Noah LSM, the model replaces the actual and saturation specific humidities with their nearly equivalent mixing ratio counterparts.

### 3.2 *Direct evaporation from bare soil*

The direct evaporation term is a simple linear relationship based on the work of Mahfouf and Noilhan (1991), who use a moisture availability parameter $\beta$ to scale the evaporation from the soil. The Noah LSM employs a similar approach based on the results from a sensitivity test for evaporation in the NCEP Eta model (Betts et al. 1997) in which

$$E_{\text{dir}} = (1-\sigma_f)\beta E_p, \tag{6}$$

where $\sigma_f$ is the fractional vegetation coverage for a model grid cell and

$$\beta = \left(\frac{\Theta_1 - \Theta_w}{\Theta_{\text{ref}} - \Theta_w}\right)^f \tag{7}$$

represents a normalized soil moisture availability term where $\Theta_w$ is the wilting point and $\Theta_{\text{ref}}$ is the field capacity, both of which depend on soil texture, and $\Theta_1$ is the volumetric water content of the top soil layer (Chen and Dudhia 2001). Some studies set $f = 1$ (e.g., Betts et al. 1997; Chen and Dudhia 2001), though in the version of the Noah LSM used here, $f = 2$ as suggested by Ek et al. (2003).

### 3.3 *Canopy transpiration*

The canopy transpiration from the vegetated portion of a model grid cell is

$$E_t = \sigma_f E_p P_c \left[1 - \left(\frac{W_c}{S}\right)^{0.5}\right], \tag{8}$$

where $W_c$ is the intercepted canopy water content and $S$ is a constant but tunable maximum canopy water capacity. The plant coefficient $P_c$ includes the influence of stomatal control and is expressed as

$$P_c = \frac{r + \Delta}{r(1 + C_h R_c) + \Delta}, \tag{9}$$

where

$$R_c = \frac{R_{\text{cmin}}}{\text{LAI} F_1 F_2 F_3 F_4} \tag{10}$$

is the canopy resistance following the formulation of Jacquemin and Noilhan (1990) where $R_{\text{cmin}}$ is the minimum stomatal resistance for each vegetation type and LAI is the leaf area index. The canopy resistance factors $F_1$, $F_2$, $F_3$, and $F_4$ are each bounded between 0 and 1 and represent the effects of solar radiation, vapor pressure deficit, air temperature, and soil moisture, respectively (Chen and Dudhia 2001). These factors are defined by

$$\begin{aligned}
F_1 &= \frac{R_{\text{cmin}}/R_{\text{cmax}} + f}{1+f} \quad \text{where } f = 0.55\frac{R_g}{R_{\text{gl}}}\frac{2}{\text{LAI}}, \\
F_2 &= \frac{1}{1 + h_s\left[w_s\left(T_0\right) - w_0\right]}, \\
F_3 &= 1 - 0.0016\left(T_{\text{ref}} - T_0\right)^2, \text{and} \\
F_4 &= \sum_{i=1}^{n} \frac{(\Theta_i - \Theta_w) d_{z_i}}{(\Theta_{\text{ref}} - \Theta_w)\left(\sum_{j=1}^{n} d_{z_j}\right)},
\end{aligned} \tag{11}$$

where $R_{\text{cmax}}$ is a constant maximum canopy resistance set to 5000 s m$^{-1}$, $R_g$ is the incoming solar radiation, $R_{\text{gl}}$ and $h_s$ are species-dependent radiation stress and empirical parameters, respectively, $w_s$ is the saturation mixing ratio at air temperature $T_0$, $w_0$ is the mixing ratio, $T_{\text{ref}}$ is 298 K as in Noilhan and Planton (1989), $\Theta$ is the volumetric water content of each soil layer, $d_z$ is the depth of each individual soil layer, and $n$ is the species-dependent number of root zone soil layers.

The canopy resistance is the most important factor contributing to canopy transpiration. Holtslag and Ek (1996) write "the [total] latent heat flux is mostly determined by the canopy resistance." Despite this physical importance, Eq. (10) that describes the canopy resistance is arguably the most questionable formulation in the Noah LSM, since it simply multiplies together four physically important atmospheric and land surface effects. Jarvis (1976) proposed a very similar formulation in an effort to forecast stomatal conductance (the inverse of which is resistance) based on the known independent influence of air temperature, leaf-air vapor pressure difference, carbon dioxide concentration, and water stress on the stomatal conductance of leaves illuminated by solar radiation. Without knowing the effect on stomatal conductance from each variable acting in concert, Jarvis (1976) hypothesized that the final stomatal conductance "is the result of complete expression of the influence of all the variables without any synergistic interactions." The final stomatal conductance is thus the product of the percentages of the maximum stomatal conductance contributed by each variable. This formulation, which sev-

eral authors have adopted and implemented in land surface models with some modification (e.g., Noilhan and Planton 1989; Jacquemin and Noilhan 1990; Chen and Dudhia 2001), leads to the canopy resistance factors that appear in Eq. (11).

### 3.4 *Wet canopy evaporation*

The evaporation of precipitation intercepted by the vegetation canopy is substantially smaller than the other evaporation terms and is

$$E_c = \sigma_f E_p \left( \frac{W_c}{S} \right)^{0.5}. \tag{12}$$

In the experiments that follow, Oklahoma Mesonet observations facilitate the development of an empirical parameterization for latent heat flux. At Oklahoma Mesonet sites, where the predominant vegetation cover is grass, it is assumed that the canopy water content is zero, thereby removing the contribution to evaporation by moisture in the vegetation canopy (cf., Betts et al. 1997). The total latent heat flux is therefore the sum of the direct evaporation and canopy transpiration terms. This is a reasonable assumption given the relative insignificance of $E_c$ compared with $E_{\rm dir}$ and $E_t$.

## 4. EMPIRICAL PARAMETERIZATION

Given the physical importance of canopy resistance in the current approach to calculating the canopy transpiration term in the Noah LSM, one technique for improving short-term latent heat flux forecasts is to focus on the formulation for canopy resistance, while leaving the remainder of the Noah LSM untouched. Driven by observations, a reversed form of the Noah LSM provides values of plant coefficient, $P_c$, and thereby canopy resistance, $R_c$, that would be necessary for the original model to yield the observed latent heat flux. Unfortunately, many of these values are unphysical, including exceedingly large canopy resistances and unbounded plant coefficients. Results indicate that this occurs because 1) the $E_{\rm dir}$ term (Eq. 6) is greater than the observed latent heat flux or 2) the sum of $E_{\rm dir}$ and $\sigma_f E_p$ (Eq. 8) in the Noah LSM is less than the observed latent heat flux, even after adjusting for a maximum $\pm$ 20 W m$^{-2}$ bias in the latent heat flux observations based on instrumentation error studies by Brotzge (2000). Thus, the direct evaporation from bare soil and canopy transpiration terms clearly yield inappropriate values when forced with observations. Any empirical scheme designed to forecast $P_c$ or $R_c$ based on these formulae would lead to poor model forecasts of latent heat flux. Improved forecasts for latent heat flux clearly require a different approach. Therefore, the popular canopy resistance approach to modeling canopy transpiration is abandoned and instead a completely new empirical latent heat flux scheme is developed from all available sets of observations. Tests indicate that least squares simple and multiple linear regression models with automatic and manual predictor selection have limited potential, though a principal-component regression procedure holds more promise as a viable alternative for predictor selection.

### 4.1 *Principal-component regression*

Meteorological data generally exhibit large spatial and temporal correlations. Least squares multiple linear regression models trained on such highly correlated data are therefore unstable and may perform poorly on independent data (Wilks 2006). These mutual correlations in the independent data can be removed through a principal component analysis, which transforms a time series of correlated variables into temporally uncorrelated, spatially orthogonal time series that remain linear functions of all the original variables. These principal components become the set of predictor variables in a least squares multiple linear regression. One benefit of using principal component analysis is that it provides an objective method for eliminating variables that are not highly correlated with any of the principal components before using those variables in a principal-component regression. Secondly, because each principal-component predictor is temporally uncorrelated with the others, elimination of any principal component as an independent variable in a multiple regression analysis does not affect the contribution of any of the other components.

Principal-component regression techniques are not new in studies of the atmosphere. Predictions of tropical precipitation from marine surface observations (Tsonis 2002), mean winter temperatures from sea-surface temperatures and pressure-surface heights (Harnack 1979), and wheat yield from temperature and rainfall observations (Wigley and Qipu 1983) have all employed this method. Air quality studies have also exercised this technique to forecast surface ozone concentrations (Pryor et al. 1995) and to determine source regions for fine particulates and sulphate (Wolff et al. 1984). However, application of this technique in an attempt to predict fluxes of latent heat from a wealth of surface observations represents a novel approach.

Since land surface models contain separate expressions for latent heat flux over bare soil and vegetated surfaces, employing separate principal-component regression analyses yields the best possible expressions for both $E_{\rm dir}$ and $E_t$ to match the observed latent heat fluxes. Training data for both $E_{\rm dir}$ and $E_t$ principal-component regressions derive from randomly selected sets of observations containing possible predictors and their respective predictands, which constitute approximately half of the available data. The remaining data are used for independent cross-validation. These independent data provide a measure of the strength of the multiple regression relationship through several measures, including the coefficient of determination $R^2$ and the residual standard error (Wilks 2006). One negative characteristic of the coefficient of determination is that its value continually increases by simply adding more variables to a prediction

equation. Thus, an adjusted $R^2$, such that

$$\overline{R}^2 = 1 - \left(1 - R^2\right)\left(\frac{n-1}{n-p-1}\right), \qquad (13)$$

instead corrects for such a problem by the inclusion of a penalty term, where $p$ is the number of predictors in the multiple regression model and $n$ is the sample size (Yamane 1967). The $\overline{R}^2$ value justifies the results of each principal-component regression in each independent cross-validation data set.

### 4.2 *Selection of observations*

Practical and physical considerations limit the range of possible predictor variables in a principal-component regression. The simplest choices for possible predictors include variables that already exist within the Noah LSM. To calculate surface energy fluxes, the model manipulates several atmospheric and soil variables determined from either internal calculations or input from the parent atmospheric model. These quantities include the downward component of both longwave and shortwave radiation, surface pressure, precipitation rate, air temperature, mixing ratio, wind speed, potential temperature, $\sigma_f$, LAI, soil temperature and soil moisture for several layers, and skin temperature. Combinations of these variables define other necessary quantities, including the saturation mixing ratio and the slope of the saturation mixing ratio curve at the current air temperature. Since the satellite-derived quantities are only available as biweekly composites, these observations require temporal interpolation to match the observation time of the Oklahoma Mesonet observations.

Data available for analysis span the period May 2004–June 2006 with satellite-derived vegetation data spanning only the period 15 April–15 September 2004. Within this time frame, there are several restrictions on the available observations from the Oklahoma Mesonet. Complete sets of quantities determining the surface energy balance are only available from nine sites. Since the latent heat flux represents the residual of the surface energy balance, the sensible heat flux, ground heat flux, and net radiation must be present in each observation record. Estimates of the storage ground heat flux require measurements of the volumetric water content at 5-cm, which is only sampled every 30 minutes. Latent heat flux observations are therefore only available at the top and bottom of each hour. Since precipitation is known to interfere with measurements from a sonic anemometer, which measures the sensible heat flux, periods of rainfall are removed from consideration beginning with the first non-zero daily precipitation total through local midnight on the day of the observation.

Sets of possible predictor variables are limited to periods with ample incoming shortwave radiation. To focus on this most important part of the day, and to limit the influence of very small nighttime latent heat fluxes in creating a new scheme for latent heat flux forecasts, the principal-component regression only considers sets of observations with incoming shortwave radiation that exceeds 10 W m$^{-2}$.

### 4.3 *Direct evaporation from bare soil*

Since vegetated surfaces surround every observation site, direct measurements of evaporation from bare soil are unavailable from the Oklahoma Mesonet. However, a long time series of soil moisture observations from May 2004 through June 2006 contains several periods during which the vegetation in Oklahoma suffered under moderate to extreme drought conditions. The permanent wilting point where transpiration ceases for most vegetation is roughly where the matric potential $\psi = -1500$ kPa (Marshall et al. 1996). At locations where the matric potential is larger in magnitude than the permanent wilting point, the only contribution to the total latent heat flux is from bare soil evaporation, assuming zero canopy water content. By separating only those sets of observations at Oklahoma Mesonet sites where the soil has reached the permanent wilting point at the 5-cm level, the residual of the surface energy balance becomes a good approximation to the direct evaporation from bare soil.

Since soil moisture observations derive from discretely observed quantities, the matric potential value that is nearest to the permanent wilting point is just under $\psi = -1490$ kPa. Therefore, a subset of the available Oklahoma Mesonet observations containing matric potentials less than $\psi = -1490$ kPa represents extremely dry soil conditions where presumably transpiration has ceased and the latent heat flux observations are equivalent to the direct soil evaporation. This subset of data comprises more than 6300 sets of observations between May 2004 and June 2006 for use in determining a new direct soil evaporation parameterization.

A substantial portion of the data during dry periods falls outside the summertime 2004 satellite measurement window. However, under the assumption that transpiration ceases when the magnitude of the matric potential exceeds the permanent wilting point, any vegetation coverage would not contribute to the total latent heat flux. The fractional vegetation coverage therefore is set to zero regardless of the availability of satellite observations.

From a wide selection of possible observable or transformed variables, multiple passes through a principal component analysis lead to a reduced pool of possible predictors for $E_{\mathrm{dir}}$. In addition to the overarching goal of achieving the largest possible adjusted $R^2$ value in the cross-validation data, several other factors contribute to the decision to retain or eliminate variables from the principal-component regression. Among these factors is the ease of implementation of the resulting flux equation in the Noah LSM. For example, matric potential holds promise as a possible predictor for latent heat flux and relates directly to water movement and plant-water uptake. Though several soil properties depend upon soil type, observations of matric potential from the Oklahoma Mesonet are independent of soil type. Includ-

ing matric potential in the Noah LSM removes an exponential dependence upon crude estimates of soil type and presumably improves the specification of water in the soil. However, results from principal-component regression tests show that replacing volumetric water content with matric potential does not generate enough improvement in $E_{\rm dir}$ forecasts to justify the difficulty of adding matric potential as a prognostic variable. Other factors include the physical relevance of each variable to evaporative processes and the statistical significance of each variable when included in a multiple linear regression. Additionally, several combinations of variables possess strong mutual correlations and must not appear together in the final regression equation. For example, the correlation coefficient between the mixing ratio and the 2-m air temperature is 0.66. Correlations are also high between incoming longwave radiation, the 2-m and 9-m air temperature, mixing ratio, saturation mixing ratio, potential temperature, and the derivative of saturation mixing ratio with respect to temperature because of the strong relationship between the air temperature and atmospheric moisture content. The existence of such highly correlated variables justifies the use of the principal-component approach in variable selection, even if the final regression equation retains all of the principal components.

The principal-component regression procedure yields a regression equation for direct evaporation from bare soil assuming that no transpiring vegetation contributes to the total latent heat flux. In practice, the fractional vegetation coverage scales the direct evaporation from bare soil. Therefore, the equation for direct evaporation from bare soil is

$$\begin{aligned} E_{\rm dir} = (&22.33 \\ &+0.0226\left[R_g\left(1-\alpha\right)\right]^{(3/2)}\left[\frac{\Theta_1-\Theta_w}{\Theta_{\rm ref}-\Theta_w}\right]^f \\ &-3.426V+3650w)\left(1-\sigma_f\right), \end{aligned} \tag{14}$$

where $R_g$ is the incoming solar radiation (W m$^{-1}$), $\alpha$ is the albedo based on the Noah LSM land use category, $\Theta_1$ is the volumetric water content (m$^3$ m$^{-3}$) at 5-cm depth, $\Theta_w$ is the wilting point and $\Theta_{\rm ref}$ is the field capacity, both of which depend on the 5-cm soil texture measured at each Oklahoma Mesonet site, $f$=1, $V$ is the 10-m wind speed (m s$^{-1}$), $w$ is the 2-m mixing ratio (kg kg$^{-1}$), and $\sigma_f$ is the fractional vegetation coverage. As implemented in the Noah LSM, $\Theta_1$ is the volumetric water content of the top soil layer, $\Theta_w$ and $\Theta_{\rm ref}$ refer to the wilting point and field capacity of the relevant gridded soil type, and $V$ and $w$ are the wind speed and mixing ratio at the lowest model level. The adjusted $R^2$ for the independent cross-validation data is 0.61, giving a correlation coefficient between forecasts and observations of 0.78, and the residual standard error is 48.4 W m$^{-2}$. By comparison, the correlation coefficient between the same predictand and the direct soil evaporation from the original Noah LSM formulation is 0.52.

As indicated by locally weighted regressions prior to the principal-component regression, each of the variables in Eq. (14) exhibits a quasi-linear relationship with the observed latent heat flux during dry conditions. The second term on the right-hand side of Eq. (14) materializes by recognizing that the available soil moisture tempers the evaporative power of the sun. An excellent linear relationship with $E_{\rm dir}$ in a locally weighted regression arises by multiplying the effective incoming solar radiation (incoming solar radiation minus outgoing solar radiation) raised to the 3/2 power by the normalized soil moisture availability term $\beta$ from Eq. (7).

With the exception of the vegetation fraction term, each term in Eq. (14) represents a single variable present in the principal component analysis. Since each component contains a very strong signal from one of each of the three variables, the final regression equation retains all three principal components. A multiple linear regression on these variables produces the same regression equation, but the large correlations between the available variables justifies using the principal-component regression approach both to ascertain the significance of the mutual correlations and as a robust variable-selection method.

Compared with the existing direct soil evaporation parameterization in the Noah LSM, the forecasts from the new empirical scheme more closely match the total latent heat flux observations when the soil is dry enough to assume senescent vegetation, particularly for increased direct soil evaporation (Fig. 1). When the soil contains sufficient moisture to support canopy transpiration, the individual contribution to evaporation from bare soil in the Noah LSM certainly should not exceed the observed total latent heat flux. Regardless of soil conditions, the new empirical scheme improves upon the original Noah LSM direct soil evaporation formulation when applied to all available sets of observations during the period 15 April–15 September 2004 by reducing substantially the frequency of unrealistic $E_{\rm dir}$ values that exceed the observed total latent heat flux.

### 4.4 *Canopy transpiration*

With a proper parameterization for the direct evaporation from bare soil in place, a similar principal-component regression procedure leads to a new empirical canopy transpiration scheme. The training and independent cross-validation data include fractional vegetation coverage and leaf area index observations spanning the period 15 April–15 September 2004. The canopy transpiration term defined by

$$E_t = \frac{E_{\rm obs}-E_{\rm dir}}{\sigma_f} \tag{15}$$

is the predictor in the multiple regression, where $E_{\rm obs}$ is the observed total latent heat flux and $E_{\rm dir}$ is the empirical direct soil evaporation term from Eq. (14) that already includes the vegetation fraction weighting.

Observed variables and those transformed based on physically plausible relationships and locally estimated

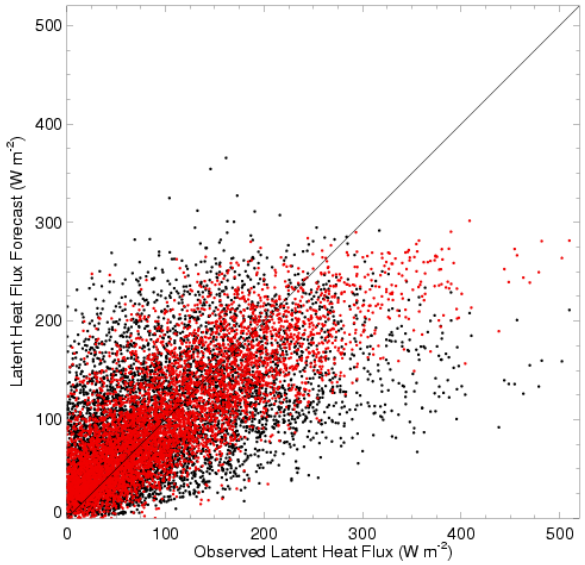


FIG. 1. Direct soil evaporation from the original Noah LSM formulation (black) and the empirical scheme (red) compared with the observed total latent heat flux under dry soil conditions.

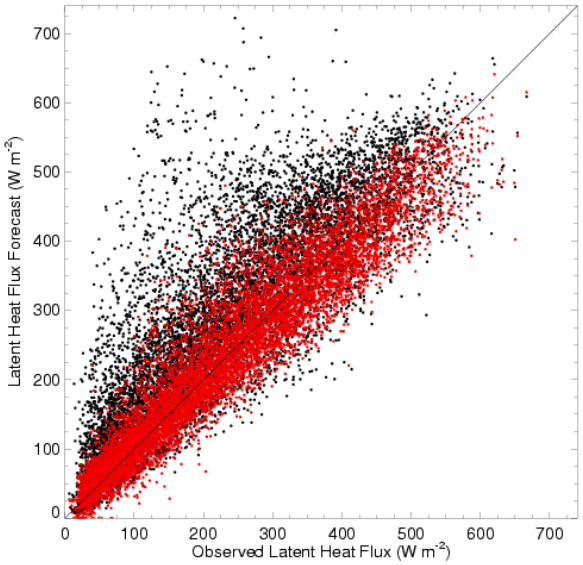


FIG. 2. Forecasts of total latent heat flux for 9239 forecast-observation pairs by the original Noah LSM formulation (black) and the new empirical direct soil evaporation and canopy transpiration schemes (red) compared with the observed total latent heat flux for the period 15 April–15 September 2004.

regressions compose a diverse set of possible forecast variables. As with the direct soil evaporation parameterization, a principal component analysis combined with physical, statistical, and practical considerations leads to the final regression equation for canopy transpiration,

$$
\begin{aligned}
E_t = \Bigg( & -1392 \\
& +0.9154 \left[ R_g (1-\alpha) \left( \left[ \frac{\Theta_3 - \Theta_w}{\Theta_{\text{ref}} - \Theta_w} \right]^{f/2} \right) \right] \\
& +4.374 T_{\text{air}} + 60.59 \left[ \frac{w}{w_s(T_{\text{air}})} \right] \Bigg) \sigma_f \\
& +6.116\,\text{LAI}, \qquad (16)
\end{aligned}
$$

where $\Theta_3$ is the volumetric water content ($\text{m}^3\ \text{m}^{-3}$) at 60-cm depth, $T_{\text{air}}$ is the 9-m air temperature (K), $w_s(T_{\text{air}})$ is the saturation mixing ratio at the 9-m air temperature ($\text{kg kg}^{-1}$), LAI is the leaf area index, and the remaining terms are the same as those defined for Eq. (14). The $\Theta_w$ and $\Theta_{\text{ref}}$ terms correspond with the measured soil textures at a depth of 60 cm at each Oklahoma Mesonet site. Observations from locations where measured soil textures are unavailable at this depth do not contribute to the training or independent cross-validation data. As implemented in the model, $\Theta_3$ is the volumetric water content of the third soil layer and $T_{\text{air}}$, $w$, and $w_s$ are the air temperature, mixing ratio, and saturation mixing ratio at the lowest model level. A large correlation for each variable corresponds with one of each of the four principal components. Therefore, the final regression equation again retains the contribution from all four principal components.

Each term in Eq. (16) represents a single variable in the principal component analysis. The leaf area index term arises by including $\text{LAI}/\sigma_f$ as a variable. The first term describes how the root-zone soil moisture availability scales the evaporative power of the sun. This is by far the dominant term in the regression equation and its inclusion supports the results of an observational study showing a strong linear relationship between root-zone soil moisture and both sensible and latent heat fluxes (Basara and Crawford 2002). The remaining air temperature, relative humidity, and leaf area index terms in the regression equation are less significant and may serve as tunable parameters for different locations. For this reason, the final regression equation retains these terms. Note, however, that Eq. (16) includes the effects of solar radiation, leaf area index, fractional vegetation coverage, vapor pressure deficit, air temperature, and soil moisture just as in the theoretical parameterization (i.e., Jacquemin and Noilhan 1990; Chen and Dudhia 2001) that appears in the original Noah LSM.

The adjusted $R^2$ for the independent cross-validation data is 0.72 and the residual standard error is 98.32 W $\text{m}^{-2}$, but recall that these numbers refer to the predictand from Eq. (15) and neglect the scaling by the fractional vegetation coverage. Using only the independent cross-validation data and summing the $E_t$ forecasts from Eq. (16) with the $E_{\text{dir}}$ forecasts from Eq. (14) to arrive at the total latent heat flux forecast, the correlation coefficient between the forecast and observed total latent heat flux is 0.94 with a residual standard error of 45.5 W $\text{m}^{-2}$.

In contrast, the correlation coefficient between the original total latent heat flux forecasts from the Noah LSM and the observed latent heat flux for the same pool of observations is 0.83 with a residual standard error of 83.8 W $m^{-2}$. Combined into a single total latent heat flux term, the empirical direct soil evaporation and canopy transpiration parameterizations vastly improve the latent heat flux forecasts by the Noah LSM when driven by observations (Fig. 2). The original parameterization tends to overestimate latent heat fluxes, while the new parameterization corrects for this problem without introducing a negative bias.

## 5. RESULTS

Several MM5 simulations initialized with satellite-derived vegetation indexes and soil temperature and moisture observations from the Oklahoma Mesonet test the effectiveness of the new latent heat flux parameterizations for the direct evaporation from bare soil and the canopy transpiration. Each model simulation also allows contributions to the total latent heat flux from the original formula for wet canopy evaporation. To explore the importance of the land surface on the model forecasts, two different sets of initial conditions for the soil and land surface initialize MM5. A control (CTRL) simulation uses climatological $\sigma_f$ and constant LAI with Eta model analyses providing the initial soil temperature and soil moisture conditions. The second initial condition (MM5VEGSOIL) includes 1-km resolution satellite-derived $\sigma_f$ and LAI with Oklahoma Mesonet observations providing the initial soil temperature and moisture conditions. When placed within the coupled MM5 model, the new latent heat flux parameterizations perform quite well for four synoptically quiescent spring and summer 2004 case studies. While daytime latent heat flux forecasts improve compared with CTRL and MM5VEGSOIL forecasts, nighttime fluxes may exceed observations by nearly 50 W $m^{-2}$, especially shortly after sunset. Limiting the selection of predictor variables to those sets of observations measured when the incoming solar radiation exceeds 10 W $m^{-2}$ in the principal-component regression constrains the resulting empirical formula. To overcome this limitation, when modeled downward shortwave radiation falls below 10 W $m^{-2}$, the latent heat flux parameterization reverts to the original canopy resistance approach.

Latent heat flux forecasts from simulations implementing the new empirical latent heat flux scheme and initialized with both satellite-derived vegetation indexes and soil temperature and moisture observations (MM5LATENT) show vast improvement over both the CTRL and MM5VEGSOIL simulations when compared with observations at Norman, Oklahoma (Fig. 3). In most cases, the model no longer severely underestimates daytime latent heat fluxes as in each of the other four MM5 simulations that use the original latent heat flux formulae with differing initial land surface and soil conditions. The MM5LATENT simulations consistently produce latent heat flux forecasts with domain-wide biases, root-mean squared errors, and mean absolute errors that are lower than or comparable to the error measures for the other forecasts.

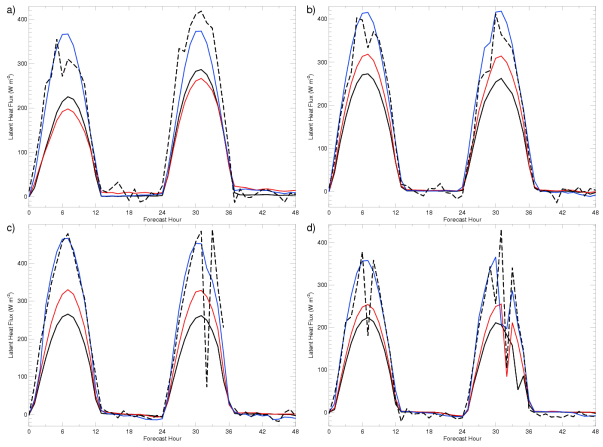


FIG. 3. Latent heat flux (W $m^{-2}$) at Norman, Oklahoma for CTRL (black), MM5VEGSOIL (red), and MM5LATENT (blue) domain four simulations initialized at 1200 UTC on a) 3 May, b) 20 July, c) 1 August, and d) 3 September 2004 compared with the residual of the surface energy balance computed from Oklahoma Mesonet observations (dashed).

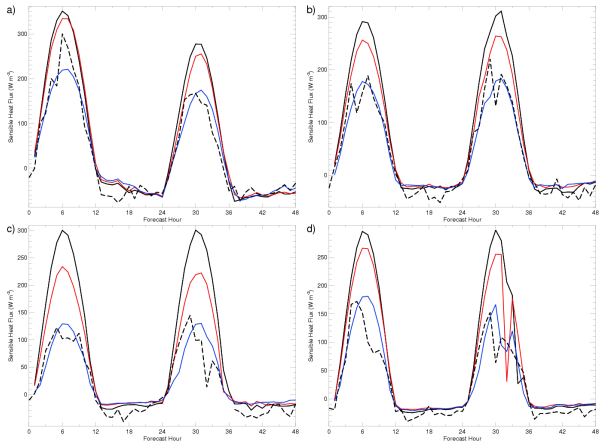


FIG. 4. Sensible heat flux (W $m^{-2}$) at Norman, Oklahoma for CTRL (black), MM5VEGSOIL (red), and MM5LATENT (blue) domain four simulations initialized at 1200 UTC on a) 3 May, b) 20 July, c) 1 August, and d) 3 September 2004 compared with Oklahoma Mesonet observations (dashed).

With reasonable latent heat flux forecasts, the previously overestimated sensible heat flux forecasts more closely resemble the observations (Fig. 4), though in each case, the model still tends to underestimate the magnitude of the observed downward sensible heat flux at night. MM5LATENT ground heat flux forecasts show little to no overall improvement over CTRL forecasts. Whether the model overestimates or underestimates the ground heat flux during the day varies by location, but the model typically overestimates the magnitude of the

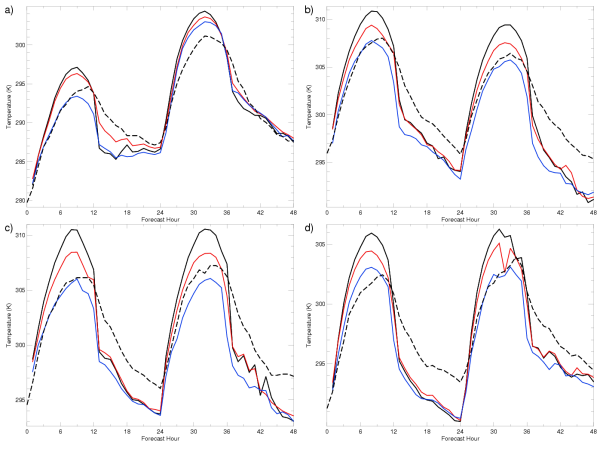

FIG. 5. 2-m air temperature (K) at Norman, Oklahoma for CTRL (black), MM5VEGSOIL (red), and MM5LATENT (blue) domain four simulations initialized at 1200 UTC on a) 3 May, b) 20 July, c) 1 August, and d) 3 September 2004 compared with Oklahoma Mesonet observations (dashed).

ground heat flux at night. Tests show that reducing the soil heat capacity in the MM5LATENT forecasts has a negligible effect on all forecast fields, so factors other than soil heat capacity errors are likely responsible for the poor ground heat flux estimates. The remaining errors in the partitioning between latent, sensible, and ground heat flux result in errors in the air temperature forecasts. While the empirical latent heat flux scheme improves the accuracy of temperature forecasts during the early morning, cumulative errors in the surface energy balance likely cause the air temperature to decrease too early in the diurnal cycle (Fig. 5). This problem appears in all forecast types. The sharp drop in 2-m air temperature near sunset is a consequence of the extrapolation errors during planetary boundary layer regime transitions and not from surface energy flux errors.

As expected, mixing ratio forecasts improve with better latent heat flux forecasts. For these four case studies, MM5 consistently underestimates the 2-m mixing ratio, regardless of the latent heat flux parameterization or initial conditions. However, with the exception of the unrealistic spike in mixing ratio values during planetary boundary layer regime transitions, mixing ratio forecast errors decrease for the MM5LATENT simulations compared with all of the other simulations (Fig. 6).

Comparisons between the model and observations across the main body of Oklahoma show similar results. However, observations from the Oklahoma Mesonet in 2004 serve as the training data for the empirical latent heat flux parameterization in the Noah LSM. Two locations outside this region provide further evidence of the ability of the new latent heat flux scheme to more accurately predict latent heat fluxes in short-term forecasts. Maintained by the United States Department of Agriculture (USDA) Agricultural Research Service (ARS) National Soil Tilth Laboratory (NSTL), these sites directly measure the four components of the surface energy balance using two meteorological-flux towers near Ames, Iowa. One tower stands over a soybean field and the other tower resides over a corn field. Roughly 2 m above the vegetation canopy at each location, Campbell Scientific CSAT3 sonic anemometers equipped with Campbell Scientific KH20 krypton hygrometers directly measure the sensible and latent heat flux using the eddy covariance method. REBS net radiometers measure the net radiation and REBS soil heat flow transducers measure the conductive ground heat flux at a depth of 6 cm with soil temperature probes buried at 2 and 4 cm to estimate the storage ground heat flux. Details of the instrumentation and site characteristics appear in Kustas et al. (2005). Data for the corn and soybean sites are available for the 20 July, 1 August, and 3 September 2004 case studies.

Since soil temperature and moisture observations are only available from the Oklahoma Mesonet, special initial conditions in the MM5LATENT forecasts only include satellite-derived vegetation indexes. As with the CTRL forecasts, the remaining initial conditions derive from Eta analyses. Despite lacking accurate initial soil temperature and moisture conditions, the 20 July and 3 August 2004 MM5LATENT simulations perform remarkably well compared with the latent heat fluxes measured over both corn and soybeans and reduce errors in the CTRL forecast by as much as 100 W m$^{-2}$ (Figs. 7–9). For these three cases, the forecasts in the CTRL simulation *overestimate* rather than underestimate the observed latent heat flux as in Oklahoma, perhaps due to cloud cover, but the new empirical latent heat flux scheme still realistically captures the total evapotranspiration at these sites. Since the gridded model results are interpolated to each flux site from a 9-km grid, the modeled fluxes over the nearly collocated corn and soybean fields are nearly identical. That fluxes measured simultaneously over the corn and soybean fields may differ by more than 100 W m$^{-2}$ highlights the variability of surface fluxes

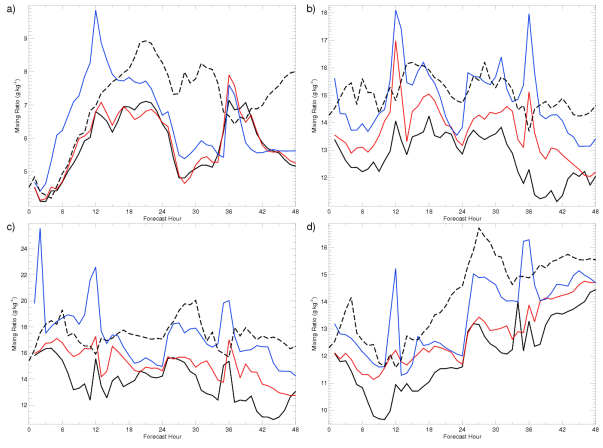

FIG. 6. 2-m mixing ratio (g kg$^{-1}$) at Norman, Oklahoma for CTRL (black), MM5VEGSOIL (red), and MM5LATENT (blue) domain four simulations initialized at 1200 UTC on a) 3 May, b) 20 July, c) 1 August, and d) 3 September 2004 compared with Oklahoma Mesonet observations (dashed).

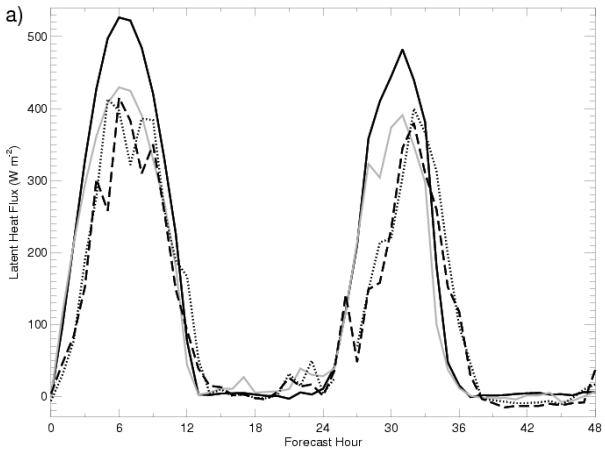


FIG. 7. Latent heat flux (W $m^{-2}$) near Ames, Iowa for CTRL (black) and MM5LATENT (gray) simulations initialized at 1200 UTC on 20 July 2004 compared with observations of latent heat flux over a soybean field (dotted) and over a corn field (dashed).

over small spatial scales as well as the difficulty of comparing gridded model output with point measurements of atmospheric fluxes. The MM5LATENT forecast underestimates the observed latent heat fluxes at each Iowa site in the forecast initialized on 3 September 2004. The corn and soybeans were not harvested until 24 and 29 September, respectively, but irrigation practices near the time of harvest could increase the available soil moisture over the fields. This increase would not appear in the soil moisture initialization from the Eta model. Additionally, the satellite-derived fractional vegetation coverage averaged over a 9 km $\times$ 9 km forecast grid includes vegetation conditions typical for early September in Iowa and may not represent the relatively small region of photosynthetically active corn and soybean fields.

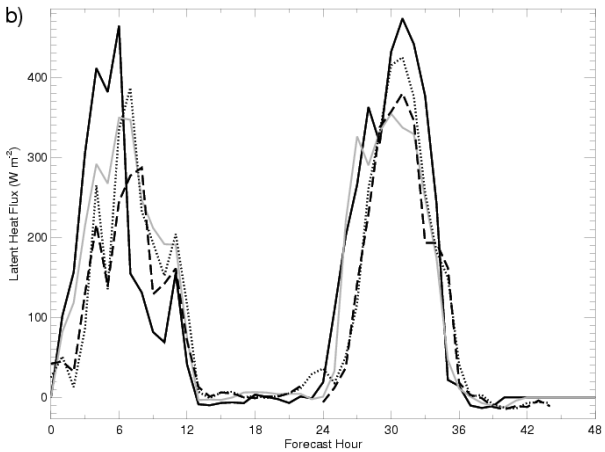


FIG. 8. As in Fig. 7 except for 1 August 2004.

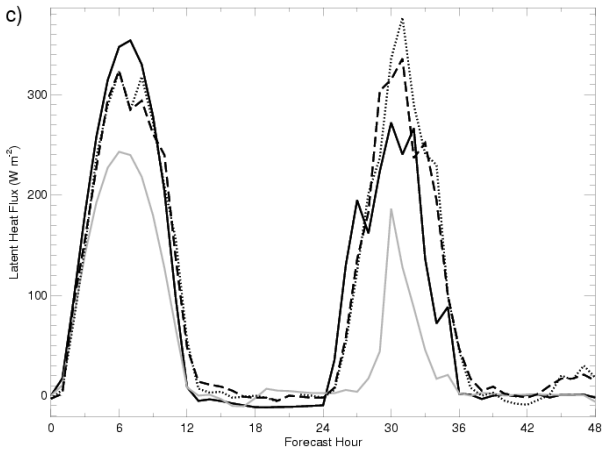


FIG. 9. As in Fig. 7 except for 3 September 2004.

## 6. DISCUSSION

While recent advances in numerical weather prediction models have led to improved short-term forecasts, land surface models still inaccurately portray near-surface conditions such as air temperature, mixing ratio, soil temperature and moisture, and surface energy fluxes. Assessing and reducing these model errors remains a difficult task because of both the wide variety of errors within the model and the lack of sufficient data for an accurate specification of the land surface. Substituting Oklahoma Mesonet observations of soil temperature and moisture and specifying vegetation conditions based on satellite observations provides a unique opportunity to begin the process of improving land surface model parameterizations by initializing the model with the best possible characterization of the land surface.

Despite providing the Noah LSM with the best possible initial conditions, the model forecasts still fail to capture realistically the surface energy fluxes that drive the evolution of the planetary boundary layer. MM5 and its companion Noah LSM in their current state produce degraded surface energy flux forecasts when compared with control forecasts and corresponding surface observations, showing that a realistic specification of land surface variables clearly affects forecast accuracy substantially. These results emphasize the significance of minimizing errors in surface initial conditions, while illustrating the profound difficulty in evaluating individual model components when all of the schemes are interdependent. Because the model physics determine the partitioning of the surface energy budget, forecast improvements for simulations with excellent soil and vegetation initial conditions require a careful calibration of many of these interdependent parameterization schemes within the Noah LSM. One new empirical parameterization determined from a wealth of unique surface, soil, and vegetation observations dramatically improves the physical representation of latent heat flux in the Noah LSM. Applying a completely new approach, this scheme replaces the usual theoretical formulations that appear in several

numerical weather prediction models.

With more detailed observations, including soil temperature and moisture at more frequent and deeper soil depths, particularly in the root zone, and direct observations of latent heat flux, an even more robust parameterization for latent heat flux could emerge. However, the new empirical scheme works well in a location far from the region where the training data were collected. This likely follows from the wide range of observations in the predictor data for the multiple linear regression. The observations from Oklahoma comprise 9-m air temperatures ranging from -10.9°C to 37.7°C, relative humidities ranging from 4% to 99%, 10-m wind speeds up to 20.3 m $s^{-1}$, mixing ratios between 0.7 and 23.6 g $kg^{-1}$, 5-cm soil volumetric water contents ranging from 0.19 to 0.42 $m^3$ $m^{-3}$, and 60-cm soil volumetric water contents ranging from 0.20 to 0.38 $m^3$ $m^{-3}$. This large span of temperature, moisture, wind, and soil conditions further indicates the applicability of the new latent heat flux parameterization to new locations across the continental United States, Canada, and Mexico. However, the behavior of the new scheme remains unclear during precipitation and when the ground lies under snow cover.

Arming MM5 with the best possible characterization of the land surface permits an assessment of the inaccuracies in the model formulations. With this information and a wealth of unique surface observations, an empirical scheme for latent heat flux emerges. Despite the dramatic improvement in latent heat flux forecasts using this empirical parameterization, nighttime latent heat fluxes require yet another approach. Here, the Noah LSM reverts to the old canopy resistance formula for determining latent heat flux at night. A different empirical parameterization based on nighttime surface energy flux observations could allow for the removal of the canopy resistance approach altogether. Continued improvement of the characterization of the land surface allows further upgrades to the Noah LSM thermodynamics and soil hydrology parameterizations and will produce more accurate forecasts of near-surface atmospheric and soil variables.

*Acknowledgments.* The authors wish to thank the Oklahoma Climatological Survey for providing Oklahoma Mesonet data and Dr. Michael Richman for his helpful comments. Funding was provided under NSF grant ATM-0243720.

REFERENCES

Basara, J. B., and T. M. Crawford, 2000: Improved installation procedures for deep-layer soil moisture measurements. *J. Atmos. Oceanic Technol.*, **17,** 879–884.

——, and K. C. Crawford, 2002: Linear relationships between root-zone soil moisture and atmospheric processes in the planetary boundary layer. *J. Geophys. Res.*, **107,** 4274, doi: 10.1029/2001JD000633.

Betts, A. K., F. Chen, K. E. Mitchell, and Z. I. Janjić, 1997: Assessment of the land surface and boundary layer models in two operational versions of the NCEP Eta model using FIFE data. *Mon. Wea. Rev.,* **125,** 2896–2916.

Bhumralkar, C. M., 1975: Numerical experiments on the computation of ground surface temperature in an atmospheric general circulation model. *J. Appl. Meteor.,* **14,** 1246–1258.

Blackadar, A. K., 1976: Modeling the nocturnal boundary layer. Preprints, *Third Symp. on Atmospheric Turbulence, Diffusion and Air Quality,* Raleigh, NC, Amer. Meteor. Soc., 46–49.

Brock, F. V., K. C. Crawford, R. L. Elliot, G. W. Cuperus, S. J. Stadler, H. L. Johnson, and M. D. Eilts, 1995: The Oklahoma Mesonet: A technical overview. *J. Atmos. Oceanic Technol.,* **12,** 5–19.

Brotzge, J. A., 2000: Closure of the surface energy budget. Ph.D. dissertation, University of Oklahoma, Norman, OK, 208 pp.

——, S. J. Richardson, K. C. Crawford, T. W. Horst, F. V. Brock, K. S. Humes, Z. Sorbjan, and R. L. Elliot, 1999: The Oklahoma atmospheric surface-layer instrumentation system (OASIS) project. Preprints, *13th Symp. on Boundary Layers and Turbulence,* Dallas, TX, Amer. Meteor. Soc., 612–615.

Chang, J.-T., and P. J. Wetzel, 1991: Effects of spatial variations of soil moisture and vegetation on the evolution of a prestorm environment: A numerical case study. *Mon. Wea. Rev.,* **119,** 1368–1390.

Chen, F., and J. Dudhia, 2001: Coupling an advanced land surface-hydrology model with the Penn State–NCAR MM5 modeling system. Part I: Model implementation and sensitivity. *Mon. Wea. Rev.,* **129,** 569–585.

——, K. Mitchell, J. Schaake, Y. Xue, H.-L. Pan, V. Koren, Q. Y. Duan, M. Ek, and A. Betts, 1996: Modeling of land-surface evaporation by four schemes and comparison with FIFE observations. *J. Geophys. Res.*, **101,** 7251–7268.

Crawford, T. M., D. J. Stensrud, F. Mora, J. W. Merchant, and P. J. Wetzel, 2001: Value of incorporating satellite-derived land cover data in MM5/PLACE for simulating surface temperatures. *J. Hydrometeor.,* **2,** 453–468.

Crook, N. A., 1996: Sensitivity of moist convection forced by boundary layer processes to low-level thermodynamic fields. *Mon. Wea. Rev.,* **124,** 1767–1785.

Deardorff, J. W., 1978: Efficient prediction of ground surface temperature and moisture, with inclusion of a layer of vegetation. *J. Geophys. Res.*, **83,** 1889–1903.

Dudhia, J., 1993: A nonhydrostatic version of the Penn State–NCAR mesoscale model: Validation tests and simulation of an Atlantic cyclone and cold front. *Mon. Wea. Rev.,* **121,** 1493–1513.

——, 2003: MM5 model status and plans. Preprints, *13th PSU/NCAR Mesoscale Model Users' Workshop,* Boulder, CO, NCAR, 1–2.

Ek, M. B., and L. Mahrt, 1991: OSU 1-D PBL model user's guide. Version 1.0.4, 118 pp. [Available from Dept. of Atmospheric Sciences, Oregon State University, Corvallis, OR 97331-2209.]

——, K. E. Mitchell, Y. Lin, E. Rogers, P. Grunmann, V. Koren, G. Gayno, and J. D. Tarpley, 2003: Implementation of Noah land surface model advances in the National Centers for Environmental Prediction operational mesoscale Eta model. *J. Geophys. Res.*, **108,** 8851, doi: 10.1029/2002JD003296.

Godfrey, C. M., D. J. Stensrud, and L. M. Leslie, 2005: The influence of improved land surface and soil data on mesoscale model predictions. Preprints, *19th Conf. on Hydrology,* San Diego, CA, Amer. Meteor. Soc., CD-ROM, 4.7.

Grell, G. A., J. Dudhia, and D. R. Stauffer, 1995: A description of the fifth-generation Penn State/NCAR Mesoscale Model (MM5). NCAR/TN-398+STR, 122 pp. [Available from MMM Division, NCAR, P.O. Box 3000, Boulder, CO 80307.]

Harnack, R. P., 1979: A further assessment of winter temperature predictions using objective methods. *Mon. Wea. Rev.,* **107,** 250–267.

Holtslag, A. A. M., and M. Ek, 1996: Simulation of surface fluxes and boundary layer development over the pine forest in HAPEX-MOBILHY. *J. Appl. Meteor.,* **35,** 202–213.

Jacquemin, B., and J. Noilhan, 1990: Sensitivity study and validation of a land surface parameterization using the HAPEX-MOBILHY data set. *Bound.-Layer Meteor.,* **52,** 93–134.

Jarvis, P. G., 1976: The interpretation of the variations in leaf water potential and stomatal conductance found in canopies in the field. *Philos. Trans. Roy. Soc. London,* **273B,** 593–610.

Jin, M., and D.-L. Zhang, 2002: Observed variations of leaf area index and its relationship with surface temperatures during warm seasons. *Meteor. Atmos. Phys.,* **80,** 117–129.

Koren, V., J. Schaake, K. Mitchell, Q.-Y. Duan, F. Chen, and J. M. Baker, 1999: A parameterization of snowpack and frozen ground intended for NCEP weather and climate models. *J. Geophys. Res.,* **104,** 19 569–19 585.

Kurkowski, N. P., D. J. Stensrud, and M. E. Baldwin, 2003: Assessment of implementing satellite-derived land cover data in the Eta model. *Wea. Forecasting,* **18,** 404–416.

Kustas, W. P., J. L. Hatfield, and J. H. Prueger, 2005: The Soil Moisture–Atmosphere Coupling Experiment (SMACEX): Background, hydrometeorological conditions, and preliminary findings. *J. Hydrometeor.,* **6,** 791–804.

Leese, J., T. Jackson, A. Pitman, and P. Dirmeyer, 2001: GEWEX/BAHC International Workshop on Soil Moisture Monitoring, Analysis, and Prediction for Hydrometeorological and Hydroclimatological Applications. *Bull. Amer. Meteor. Soc.,* **82,** 1423–1430.

Mahfouf J.-F., and J. Noilhan, 1991: Comparative study of various formulations of evaporation from bare soil using in situ data. *J. Appl. Meteor.,* **30,** 1354–1365.

Mahrt, L., and M. Ek, 1984: The influence of atmospheric stability on potential evaporation. *J. Climate Appl. Meteor.,* **23,** 222–234.

Marshall, T. J., J. W. Holmes, and C. W. Rose, 1996: Soil Physics. 3d ed. Cambridge University Press, 453 pp.

Matsui, T., V. Lakshmi, and E. E. Small, 2005: The effects of satellite-derived vegetation cover variability on simulated land-atmosphere interactions in the NAMS. *J. Climate,* **18,** 21–40.

McCumber, M. C., and R. A. Pielke, 1981: Simulation of the effects of surface fluxes of heat and moisture in a mesoscale numerical model. *J. Geophys. Res.,* **86,** 9929–9938.

Noilhan, J., and S. Planton, 1989: A simple parameterization of land-surface processes for meteorological models. *Mon. Wea. Rev.,* **117,** 536–549.

Oleson, K. W., and G. B. Bonan, 2000: The effects of remotely sensed plant functional type and leaf area index on simulations of boreal forest surface fluxes by the NCAR land surface model. *J. Hydrometeor.,* **1,** 431–446.

Pan, H. L., and L. Mahrt, 1987: Interaction between soil hydrology and boundary-layer development. *Bound.-Layer Meteor.,* **38,** 185–202.

Penman, H. L., 1948: Natural evaporation from open water, bare soil and grass. *Proc. Roy. Soc. London,,* **193A,** 120–145.

Pryor, S. C., I. G. McKendry, and D. G. Steyn, 1995: Synoptic-scale meteorological variability and surface ozone concentrations in Vancouver, British Columbia. *J. Appl. Meteor.,* **34,** 1824–1833.

Robock, A., K. Y. Vinnikov, G. Srinivasan, J. K. Entin, S. E. Hollinger, N. A. Speranskaya, S. Liu, and A. Namkhai, 2000: The global soil moisture data bank. *Bull. Amer. Meteor. Soc.,* **81,** 1281–1299.

Santanello, J. A., and T. N. Carlson, 2001: Mesoscale simulation of rapid soil drying and its implications for predicting daytime temperature. *J. Hydrometeor.,* **2,** 71–88.

Shafer, M. A., C. A. Fiebrich, D. S. Arndt, S. E. Fredrickson, and T. W. Hughes, 2000: Quality assurance procedures in the Oklahoma Mesonetwork. *J. Atmos. Sci.,* **17,** 474–494.

Tsonis, A. A., 2002: The problem of extracting precipitation information in the tropics from the UWM/COADS data. *J. Appl. Meteor.,* **41,** 1153–1162.

Viterbo, P., and A. C. M. Beljaars, 1995: An improved land surface parameterization scheme in the ECMWF model and its validation. *J. Climate,* **8,** 2716–2748.

Wei, M.-Y., Ed., 1995: Soil Moisture: Report of a Workshop Held in Tiburon, California, 25–27 January 1994. NASA Conference Publication 3319, 80 pp.

Wigley, T. M. L., and T. Qipu, 1983: Crop-climate modeling using spatial patterns of yield and climate. Part 1: Background and an example from Australia. *J. Climate Appl. Meteor.,* **22,** 1831–1841.

Wilks, D. S., 2006: *Statistical Methods in the Atmospheric Sciences.* International Geophysics Series, Vol. 91, Academic Press, 627 pp.

Wolff, G. T., M. L. Morrissey, and N. A. Kelly, 1984: An investigation of the sources of summertime haze in the Blue Ridge Mountains using multivariate statistical methods. *J. Climate Appl. Meteor.,* **23,** 1333–1341.

Yamane, T., 1967: *Statistics, an introductory analysis.* 2d ed. Harper and Row, 919 pp.

Zeng, X., R. E. Dickinson, A. Walker, M. Shaikh, R. S. DeFries, and J. Qi, 2000: Derivation and evaluation of global 1-km fractional vegetation cover data for land modeling. *J. Appl. Meteor.,* **39,** 826–839.